Discretization of Concrete Behavior into Four Planar Cases by Elastoplastic Multiplane Model

A.A.Khosroshahi[1], S.A.Sadrnejad[2]

[1]Ph.D Candidate

[2]Professor

Department of Civil Engineering,K.N.Toosi University of Technology,Tehran, Iran.

Abstract:*A framework for development of constitutive models including damage progress, based on semi-micromechanical aspects of plasticity is proposed for concrete. The model uses sub-loading surface with multilaminate framework to provide kinematics and isotropic hardening/softening in the ascending/descending branches of loading and can be able to keep stress/stain paths histories for each plane separately. State of stresses on planes is divided to four basic stress patterns i.e. pure compression, increasing compression-and shear, decreasing compression-shear and tension-shear and used in derivation of plasticity equations. Under this kind of categorized form the model is capable of predicting behavior of concrete under any stress/strain path such as uniaxial, biaxial and triaxial in the monotonic and cyclic loading, Also this model is capable of predicting the effects of principal stress/strain axes rotations and consequent plastic flow and has the potential to simulate the behavior of material with anisotropy, fabric pattern, slip/weak planes and crack opening/closing. The material parameters of model are calibrated by optimum fitting of the basic test data available in the literature. The model results under both monotonic and cyclic loading have been compared with experimental results to show capability of model.*

1. Introduction

A simulation of fractured mechanism of concrete has been implemented in elastoplastic model. For proper analysis, modeling of behavior of concrete under different states of multiaxial stresses, load paths especially in the post-peak region and prediction of aspects such as unloading/reloading are very significant. The other cases of research are the behavior after crack and splitting where concrete behavior is anisotropy. Several models are used in the recent years based on the stress/strain invariants, but the classical approach to constitutive modeling of concrete based on direct use of stress/strain tensor and their invariants which were used in the first decade of computer programming, now there is not led to more accurate modeling of concrete, However the models based on the concrete microstructures such as microplane and multilaminate can be able to improve concrete modeling specially where the concrete is non-isotropic or where there is fabric property or crack in the concrete. The proposed model is able to predict the behavior of concrete under any arbitrary stress/strain path and final failure mechanism.

1.1 History of multilaminate

The concept of multilaminate approach was firstly proposed by Taylor in 1938[34].Later a theory of plasticity based on the concept of slip theory was developed by Batdorf and Budiansky[35] for metals. This theory was based on the assumption that slip in any particular orientation in the material develops a plastic shear strain which depends only on the history of the corresponding component of shear stresses/strains .Multilaminates model for rocks was developed by Zienkiewicz and Pande[30],Also Pande and Sharma[31]developed elastoviscoplastic model for clays.

Bazant and Oh[32] developed a model

named as microplane model for fracture analysis of concrete. This model was based on the strain control parameters. Sadrnejad[33] developed a multilaminate model for granular materials.

The concept of multilaminate is based on the numerical approximation of integration of a certain physical property distribution such as strain distributed over the surface of a media. This approach can be numerically achieved by summing up the multiplication of the property values by the specified weighted coefficients at predefined points and considering it as an approximate representative value over the media, Based on this framework the behavior of a three dimensional media is averaged and approximated into the appropriate summation of slipping behavior of sampling planes passing through points. Consequently, this slip feature could be representative of the real variations of strain are taken place through the boundaries of artificial structural units. Therefore, the preciseness of the solutions is highly related to employed constitutive relation for frictional slip/opening/closing gaps of a sampling point.

2. Model explanation

The proposed model is originally based on the multi-laminate framework for elastoplastic behavior of intact concrete substructural boundaries, considering hardening/softening rule and elastic behavior of substructural units. It consists following bases:

- Constitutive equations
- Yield function and potential surface
- Hardening/Softening rule
- Flow rule and consistency condition

- Different crack initiation and contraction effects

2.1 General Constitutive equation

From classical theory strain can be decomposed to elastic and plastic components as follows:

$$d\varepsilon = d\varepsilon^e + d\varepsilon^P \qquad (1)$$

$$d\varepsilon^e = C^e d\sigma \qquad (2)$$

$$d\varepsilon^P = C^P d\sigma \qquad (3)$$

C^e is the elastic part of compliance matrix and C^P is the plastic compliance matrix. C^e is constant for different planes and is computed from elasticity theory.

$d\varepsilon^P$ Can be calculated from weighted summation of $d\varepsilon_i^p$ of active planes, for sphere with n planes with considering multilaminate approach:

$$d\varepsilon^P = 8\pi \sum_{i=1}^{n} W_i [L_\varepsilon]^T . d\varepsilon_i^p \qquad (4)$$

And $d\varepsilon_i^p = \overline{C}_i^p d\sigma_i$

$$d\varepsilon^P = 8\pi \sum_{i=1}^{n} W_i [L_\varepsilon]^T . \overline{C}_i^p . [L_\sigma] d\sigma \qquad (5)$$

$$C_i^p = [L_\varepsilon]^T . \overline{C}_i^p . [L_\sigma] \qquad (6)$$

$$C^P = 8\pi \sum_{i=1}^{n} W_i . C_i^p . \qquad (7)$$

Where L_e and L_s are transformation matrices for strain and stresses, respectively and n is number of planes. $\overline{C}_i^p$ is 3×3 compliance matrix for plane i in the local coordinates and C_i^p is 6×6 compliance matrix in the global coordinate.

C^P is composed from weighted summation of C_i^p corresponding to any of the active

Fig.1 Multilaminate planes orientations

Fig.2 Normal-yield and Subloading surfaces

planes, It should be noted that C_i^p for elastic planes(Non-active planes) is equal ZeroThe procedure for calculation of C_i^p is presented in section 3, Analysis shows that using 13 planes satisfy accuracy for most engineering problems. These planes are shown in the Figure 1.

A modified Sub-loading yield surface is used in the models[21],for elasto-plastic behavior of planes as shown in the figure 2 subloading surface always passes through the current stress point and also keeps a similar shape to the yield surface, renamed as the normal-yield surface, and an orientation of similarity

to the normal-yield surface. Then, the subloading surface does not only translate but expands/contracts with the plastic deformation. The similarity-center S moves with a plastic deformation describes the back stress in loading/unloading, although it was fixed in the origin of stress space in the initial subloading surface model, Vector represents the kinematic hardening vector and is the vector normal to subloading and yield surface that with some modification as shown in section 3 shows the direction of strain rate,with using this concept the model has strong capability to predict isotropic and kinematics hardening behavior for loading, unloading and reloading

2.2 The Basic Planar Cases

The effects of any stress/strain path over a simple typical dx, dy, dz cube element on an arbitrary sampling plane can be led to four stress/strain patterns. All of stress states in the material can be divided to these four categories on a typical plane as follows:

- Compression –shear with increasing in the compression
- Compression –shear with decreasing in the compression
- Tension –shear
- Pure compression

In this framework any form of yield criterion including crack effects may be for different sampling plane to consider any local behavior aspect and with the summation of all planes behavior we can approach to media behavior.

In the most cases of element stress/strain paths the compression or tension accompanied with shear is governing case but for generality of model pure compression is considered in the model. In this way any complex form of stress/strain path is

analysed into the stated four cases on planes and lead to proper planar behavior
The yielding criteria proposed for the identified cases are introduced as follow :

2.2.1 Compression-Shear

When a plane is subjected to compression and shear two load paths may exist:

1. Increasing or constant shear/compression rate with increase in the compression stress, sample of this load path is Triaxial compression test with constant lateral pressure and increasing axial compression stress, The uniaxial compression is a special case that shear/compression ratio is constant.

2. Increasing shear/compression rate with decreasing compression stress, sample of this load pattern is triaxial test when the lateral compression is decreased but axial compression is remained.

The behavior of concrete under the above load paths is not completely similar thus two separate functions are used in the equations.

2.2.1.1 Increasing shear/compression rate with increase in the compression stress

In this model hyperbolic yield function for compressive and shear stresses is considered as follows:

$$f(\hat{\sigma}) = \tau - C_H(\sigma_n + C_3\sigma_n^2) - F(H) \qquad (8)$$

$$\tau = \sqrt{\hat{\sigma}_y^2 + \hat{\sigma}_z^2} \qquad (9)$$

$$\sigma_n = \sigma_x \qquad (10)$$

C_3 = Material constant
F(H) = Hardening/Softening Function

$$F(H) = v_2(1 + C_1(H_i / H_m) + v_4$$
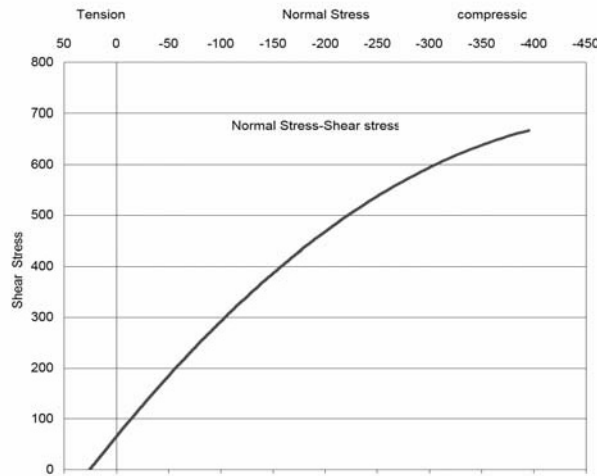$$, \ H_i \le H_m \qquad (11)$$

Fig.3 Typical yield function for compression /Tension Shear

$$F(H) = v_2(1 + C_1(H_i/H_m) + v_2.C_2(H_i/H_m - 1) + v_4$$

$$, \quad H_i > H_m \tag{12}$$

$$H_i = \sqrt{\varepsilon_{xi}^{p^2} + \varepsilon_{yi}^{p^2}} + \varepsilon_{zi}^{p^2} \quad \text{Plastic strain} \tag{13}$$

H_m ,v_1 =Material variable parameter
C_1,C_2 Material fixed parameters
$\mathbf{v}_2$ Material Strength variable
C_{Hi} Hystersis softening parameter

$$C_{Hi} = v_3.e^{A_i(H_i - H_{0i})} - (SIGN.v_3 - C_{H0i})e^{A_i(H_i - H_{0i})}$$
$$- C_{11}(1 - SIGN)(C_4.v_3 - C_{h0i})e^{A_i(H_I - H_{0i})} \tag{14}$$

SIGN= 1 for loading/reloading,
SIGN= -1 Unloading
C_{H0i} value of C_{Hi} at the end of previous cycle, For First loading it may be $C_{H0i} = v_3.C_4$
H_{0i} value of H_i at the end of previous cycle in the first loading(virgin material) it is zero. If the previous load path is pure compression $H_{0i} = C_{14}\varepsilon_{v\,max}$
A_i Cyclic parameter, at the first loading it is C_{12}, then it becomes :

$$A_i = C_{12} + C_{13}H_{0i} \tag{15}$$

at the end of previous cycle

All of active planes in the states of loadings such as uniaxial compression, Biaxial Compression, Triaxial Compression and some of planes in the Biaxial Compression-Tension test can be categorized in the compression-Shear state .Also it should be noted that some of planes, for example plane normal to load in uniaxial compression test is in pure compression but this plane remain elastic in the test.Fig. 3 shows the typical yield function for compression /Tension Shear.

2.2.1.2 Increasing shear/compression rate with decrease in compression stress

In the model yield function is similar to increasing compression stress except the C_3 is revised to C_5 as follows:

$$f(\hat{\sigma}) = \tau - C_H(\sigma_n + C_5\sigma_n^2) - F(H) \tag{16}$$

2.2.2 Tension-Shear

In this model mohr-Coloumb linear yield function between tension stress and shear stress is used:
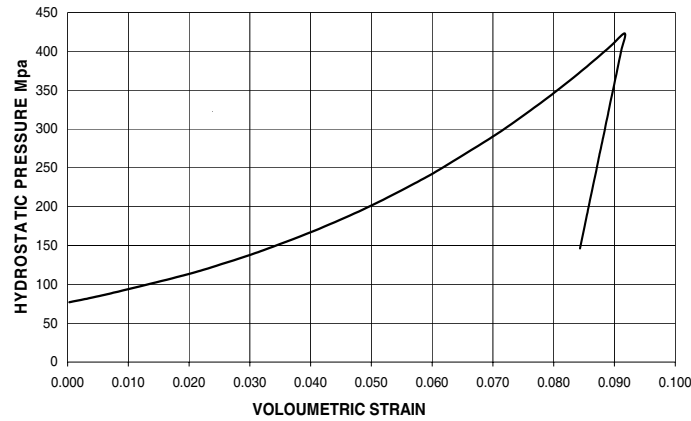
$$f(\hat{\sigma}) = \tau - C_H\sigma_n - F_T(H) \tag{17}$$

Fig.4 Pure compression yield function

$$\tau = \sqrt{\hat{\sigma}_y^2 + \hat{\sigma}_z^2} \tag{18}$$

$$\sigma_n = \sigma_x \tag{19}$$

$$F_T(H) = (v_2 + v_4)e^{C_8 H_i} \tag{20}$$

Hardening is considered in the C_H as frictional hardening/softening including degrading in the cyclic hystersis behavior also $F_T(H_i)$ represents cohesional hardening/softening and when the crack opens the cohesional strength of material is considered as zero but the frictional strength is remained.

2.2.3 Pure compression state

For pure compression exponential function is used as follows:

$$\sigma_n = E_c v_5 Exp(-C_9 \varepsilon_v) - E_c v_5 \tag{21}$$

$$f(\hat{\sigma}) = -\sigma_n + v_5 E_c Exp(-C_9 \varepsilon_v) - E_c v_5 \tag{22}$$

$$\varepsilon_v = (\varepsilon_n + \varepsilon_y + \varepsilon_z)/3 \tag{23}$$

$\varepsilon_{v\,max} = Max\varepsilon_v$ at end of loading
C_9 = Material fixed parameter
v_5 = Material variable parameter

Fig. 4 Shows this function typically.

2.3 Stresses on planes

For plane i three normal vectors is defined and stress is computed as follow:

σ_i = stress on plane i
$\vec{n}_i$ = normal cosine of plane i
$\vec{m}_i$ = Arbitrary vector on plane i
$\vec{l}_i$ = Vector on plane i perpendicular $\vec{m}_i$
Vector summaries are as shown in Table 1.

2.4 Kinematic Hardening

Kinematic hardening is defined as below:

$$\hat{\sigma}_i = \sigma_i - \alpha_i \tag{24}$$

$\hat{\alpha}_i$ = Kinematics hardening vector

$$\hat{\alpha}_i = b_i \frac{\sigma_i}{\|\sigma_i\|} \tag{25}$$

$$b_i = C_6 H_i^{c_7} \tag{26}$$

C_6, C_7, material constants

3. Computation procedure

After calculation of stress and yield function for guaranty to move in or at the surface of

Table1 Plane vectors cosine direction and weight

Plane	$\vec{n}$	$\vec{m}$	$\vec{l}$	Weight
1	$\frac{1}{\sqrt{3}}, \frac{1}{\sqrt{3}}, \frac{1}{\sqrt{3}}$	$\sqrt{\frac{1}{2}}, -\sqrt{\frac{1}{2}}, 0$	$-\sqrt{\frac{1}{6}}, -\sqrt{\frac{1}{6}}, 2\sqrt{\frac{1}{6}}$	27/840
2	$\frac{1}{\sqrt{3}}, -\frac{1}{\sqrt{3}}, \frac{1}{\sqrt{3}}$	$\sqrt{\frac{1}{2}}, \sqrt{\frac{1}{2}}, 0$	$\sqrt{\frac{1}{6}}, -\sqrt{\frac{1}{6}}, -2\sqrt{\frac{1}{6}}$	27/840
3	$-\frac{1}{\sqrt{3}}, \frac{1}{\sqrt{3}}, \frac{1}{\sqrt{3}}$	$\sqrt{\frac{1}{2}}, \sqrt{\frac{1}{2}}, 0$	$+\sqrt{\frac{1}{6}}, -\sqrt{\frac{1}{6}}, +2\sqrt{\frac{1}{6}}$	27/840
4	$-\sqrt{\frac{1}{3}}, -\sqrt{\frac{1}{3}}, \sqrt{\frac{1}{3}}$	$\sqrt{\frac{1}{2}}, -\sqrt{\frac{1}{2}}, 0$	$-\sqrt{\frac{1}{6}}, -\sqrt{\frac{1}{6}}, -2\sqrt{\frac{1}{6}}$	27/840
5	$+\sqrt{\frac{1}{2}}, \sqrt{\frac{1}{2}}, 0$	$\sqrt{\frac{1}{2}}, -\sqrt{\frac{1}{2}}, 0$	$0, 0, 1$	32/840
6	$-\sqrt{\frac{1}{2}}, \sqrt{\frac{1}{2}}, 0$	$\sqrt{\frac{1}{2}}, \sqrt{\frac{1}{2}}, 0$	$0, 0, 1$	32/840
7	$+\sqrt{\frac{1}{2}}, 0, \sqrt{\frac{1}{2}}$	$\sqrt{\frac{1}{2}}, 0, -\sqrt{\frac{1}{2}}$	$0, 1, 0$	32/840
8	$-\sqrt{\frac{1}{2}}, 0, \sqrt{\frac{1}{2}}$	$\sqrt{\frac{1}{2}}, 0, \sqrt{\frac{1}{2}}$	$0, 1, 0$	32/840
9	$0, -\sqrt{\frac{1}{2}}, \sqrt{\frac{1}{2}}$	$0, \sqrt{\frac{1}{2}}, \sqrt{\frac{1}{2}}$	$1, 0, 0$	32/840
10	$0, \sqrt{\frac{1}{2}}, \sqrt{\frac{1}{2}}$	$0, -\sqrt{\frac{1}{2}}, -\sqrt{\frac{1}{2}}$	$1, 0, 0$	32/840
11	1 , 0 , 0	0 , 1 , 0	0 , 0 , 1	40/840
12	0 , 1 , 0	1 , 0 , 0	0 , 0 , 1	40/840
13	0 , 0 , 1	0 , 0 , 1	1 , 0 , 0	40/840

yield function a penalty function of U is defined as:

$$R_i = \frac{f_i(\hat{\sigma}_i)}{F_i(H_i)} \leq 1.0 \tag{27}$$

$$U_i = -u_i \ln R_i \tag{28}$$

$u_i = V_6$ Material variable parameter for shear compression state
$u_i = V_7$ Material variable parameter for shear tension state

U is the function that relates R increment to plastic strain increment and it guarantees that Ri to be less than unit, It should be noted that in the numerical calculation R may be greater than one for 1-2 steps but the penalty function of U adjust it to unit even though the load step is large.

$$\dot{R}_i = U_i \| d\varepsilon_i^p \| \tag{29}$$

$u = \infty$ for   R = 0
$u > 0$ R < 1
$u = 0$ R = 1
$u < 0$ R > 1

Similarity center S is the center of subloading in the space of stress

$$S_i^{k+1} = S_i^k + \dot{S}_i \tag{30}$$

$$\dot{S} = C_{10} \| d\varepsilon^p \| \frac{\tilde{\sigma}_i}{R_i} + \dot{\alpha} + \frac{1}{F} \left\{ \overset{0}{F} \hat{S} \right\} \tag{31}$$

C_{10} = material constant

$$\tilde{\sigma}_i = \sigma_i - S_i \tag{32}$$

$$\hat{S} = S_i - \alpha_i \tag{33}$$

$$d\varepsilon^P = \lambda \overline{N}_{NA} \quad \text{Non Associate flow rule} \tag{34}$$

$$\overline{N} = \frac{\partial f(\overline{\sigma})}{\partial \sigma} / \| \frac{\partial f(\overline{\sigma})}{\partial \sigma} \| \quad \| \overline{N} \| = 1 \tag{35}$$

$$\overline{N}'_{NA}(1) = \frac{\partial f(\overline{\sigma})}{\partial \sigma} . C_{15} \quad ,$$

$$\overline{N}'_{NA}(2) = \frac{\partial f(\overline{\sigma})}{\partial \sigma} \quad , \tag{36}$$

$$\overline{N}'_{NA}(3) = \frac{\partial f(\overline{\sigma})}{\partial \sigma}$$

Table 2 Variable Parameters range

Variable Parameter	Minimum Value	Maximum Value	Recommended Value(f'c=40MPa)	Unit
V_1	.0005	0.05	0.01	m
V_2	0.2E7	0.5E7	0.3E7	Pa
V_3	0.55	0.7	0.63	-
V_4	0.05E7	0.2E7	0.1E7	Pa
V_5	-.002	-.005	-.003	-
V_6	3,000	8,000	5,000	-
V_7	100,000	150,000	120,000	-

$$\overline{N}_{NA} = \overline{N}'_{NA} \, / \, \|\overline{N}'_{NA}\| \qquad (37)$$

C_{15} = Material constant

$$d\varepsilon^P = \frac{tr(\overline{N}\dot{\sigma})}{\overline{M}_P} \overline{N}_{NA} \qquad (38)$$

$$\overline{M}^P = tr\left[\overline{N}\left[\overline{a} + \left[\frac{F'}{F}h + \frac{U}{R} \right]\overline{\sigma} \right] \right] \qquad (39)$$

$$h = \frac{\dot{H}}{\lambda} \qquad , \qquad a = \frac{\dot{\alpha}}{\lambda}$$

$$\overline{a} = \frac{\dot{\alpha}}{\lambda} = (1-R)Z - U\hat{S} + Ra \qquad (40)$$

$$Z = \frac{\dot{S}}{\lambda} = C\frac{\tilde{\sigma}}{R} + a + \frac{1}{F}F'h\hat{S} \qquad (41)$$

$$C_i^p = \frac{tr(\overline{N}_i \dot{\sigma}_i)}{\overline{M}_i^p} N_{NAi} \qquad (42)$$

Then the C^p can be calculated with weighted summation of all planes.

$$C^p = 8\pi \sum_{i=1}^{13} w_i C_i^p \qquad (43)$$

4. Calibration

The parameters of models are divided into two groups, fixed parameters that are same for all normal concretes and need not to be calibrated for any concrete, They are parameters $C_1, C_2, ..., C_{15}$, and variable parameters that should be adjusted for specified concrete such as $V_1, V_2, ..., V_7$.

The model has been calibrated for experimental data in three stages, in the first stage the material strengths under different classical load paths such as biaxial stresses, uniaxial compression and tension, triaxial compression and shear –compression interaction are evaluated and most of material parameters are defined, at the second stage the material response and strain are evaluated for many load paths such as uniaxial compression, uniaxial tension,biaxial compression, biaxial compression-tension,triaxial compression with increase in axial compression or decrease in lateral pressure and also concrete behavior under pure compression, In the last stage the model is evaluated for unloading,reloading and cyclic loading in the uniaxial compression.

For calibration of variable parameters (V_1 to V_7)that have more effects on the model behavior, specified concrete stress-strain data for uniaxial compression,uniaxial tension and also a data for biaxial or Triaxial compression strength are necessary for calibration of shear-compression and shear-tension states and test data for pure compression should be used for calibration of model if pure compression is important. The variable parameters ranges are as shown in Table 2 (SI units).

The effect of each variable parameter on the

Table 3 Fixed Parameters

Fixed Parameter	Recommended Value (Normal Concrete)	Unit
C_1	-0.01	-
C_2	-0.001	-
C_3	3.E-9	Pa^{-1}
C_4	1.8	-
C_5	1.5E-9	Pa^{-1}
C_6	1.6E6	Pa
C_7	0.4	-
C_8	5000	m^{-1}
C_9	250.	m^{-1}
C_{10}	300	Pa
C_{11}	200	-
C_{12}	-55.	m^{-1}
C_{13}	-5000.	m^{-2}
C_{14}	0.11	-
C_{15}	0.20	-

model behavior is investigated by sensitivity analyses and results are as follow:

V_1 Shifts peak stress, increase strain over peak stress point

V_2 Increase concrete strength, specially shear and tensile strength

V_3 Changes stiffness and also compression strength

V_4 controls on the pure shear strength and tensile strength

V_5 Increase material strength and stiffness in pure compression

V_6 Controls material stiffness in the compression state

V_7 Controls material stiffness in the tension state

Fixed parameters (C_1 to C_{15}) have not changed in the different concrete and the values which were set can be used for normal concrete with compressive strength between 20MPa to 60 MPa but for high strength concrete or special concrete such as fiber reinforced concrete these value should be adjusted, It should be noted that when more preciseness is necessary some of the fixed parameter is recommended to be adjusted for example $C3$ is very important for high confinement or C_{13} is very important for cyclic stress behavior. The typical values of fixed parameters for normal concrete are as show in Table 3.

The effects of each fixed parameter on the model behavior are investigated and are as follow:

C_1, C_2 Shift post peak and effect on the residual stress and stiffness on the postpeak

C_3 Controls strength on high pressure region specially (increasing compression)

C_4 Controls stiffness degrading

C_5 Controls strength on high pressure region specially (Decreasing compression)

C_6, C_7 Affect on the kinematic hardening
C_8 Affect on the hardening/softening in the tension state(post peak)
C_9 Control the plastic curvature in pure compression
C_{10} Control hystersis behavior and residual stress
C_{11} Affect on the back stress in the hystersis loading,
C_{12} and C_{13} affect on the hystersis behavior
C_{14} Relates the pure compression damage to other states of stress
C_{15} Affect on the volumetric strain
It should be noted that if only compression-shear state is important the strength of concrete can be adjusted with defining V_2 and V_3 and for strength calibration, V_6 for adjusting Stiffness and V_1 for post peak region if it is needed, Thus for compression shear state in the ascending branch of loading that is most important and practical case only three variable of V_2, V_3 and V_6 calibration are necessary, For more preciseness near peak and over V_1 should be adjusted, For tension and tension shear cases variable V_3, V_4 and V_7 should be adjusted too. V_5 adjustment is only necessary for pure compression or high confinement pressure.

5. Model Evaluation

As illustrated above the model has been evaluated with experimental data from literature for its calibration and evaluations Figure 5 shows the comparison of shear compression stress interaction of model prediction with as experimental test of by Bresler[24]that shows the strength of model is close to experimental result.

Figure 6 shows the biaxial stress envelop of Tasuji[29] with model prediction,the model has good fitting in compression-tension and

also tension-tension region but in the compression-compression region it is little more than experimental result.

Figure 7 shows the result of uniaxial compression test(Van Mier[26])with as predicted by model that shows very good fitting of whole response, also the volumetric strain result of model is compared with experimental data that is quite fitted.

Figure 8 shows the comparison of uniaxial tension tests performed by Pettersson[26],the model result is close to experimental data and has good fitting.

Figures 9 and 10 show the experimental data of Sfer[6] for high and low lateral pressure of triaxial test with model result, they show that model predicts higher strength in high pressure (7%) but in the lower pressure it is close to experimental result.

Figure 11 shows the result of triaxial compression test data where the lateral pressure decreased and axial pressure increased with ratio of 1/-0.2,then after peak the axial pressure drops(unloading),The model prediction has good fitting with the experimental data[4].

Figure 12 show the result of hydrostatic compression of Green and Swanson[22] with model prediction that shows very good fitting of model and experimental data.
Figures 13 and 14 show the comparison between Tasuji[29] test data for biaxial compression-compression and biaxial compression-tension, it should be noted that the model and test data is close near peak but model predicts higher strength.

Figure 15 show the result of uniaxial compression cyclic loading of Sinha[28] with model prediction that shows close fitting
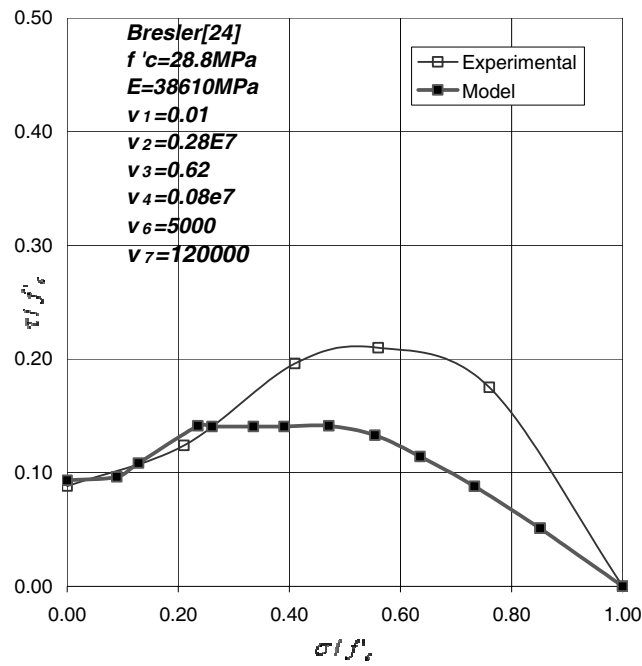
Fig.5 Comparison of model for shear-compression experimental data,Bresler[6]
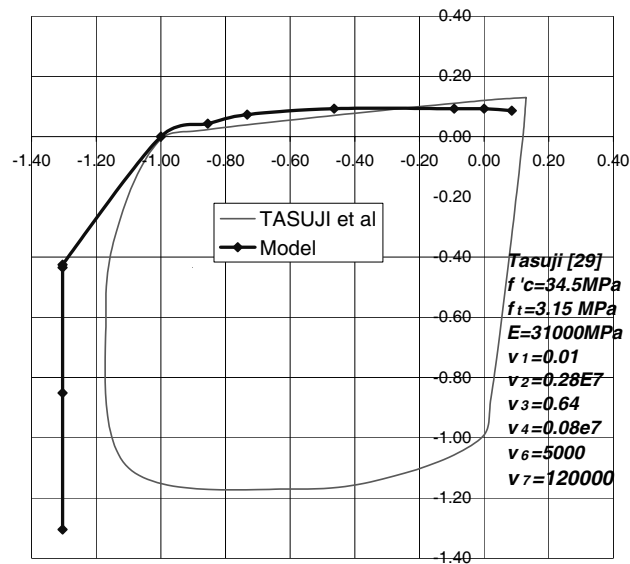

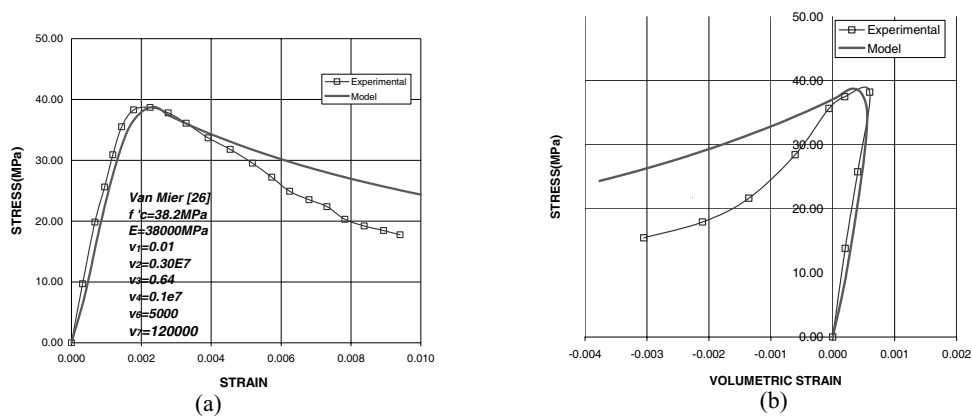**Fig.6** Comparison of model for biaxial stress experimental data,Tasuji[29]

58

International Journal of Civil Engineerng. Vol. 5, No. 1, March 2007

Fig.7 Comparison of model for uniaxial compression experimental data,Van mier[26] a)Stress-strain curve b)volumetric strain versus stress
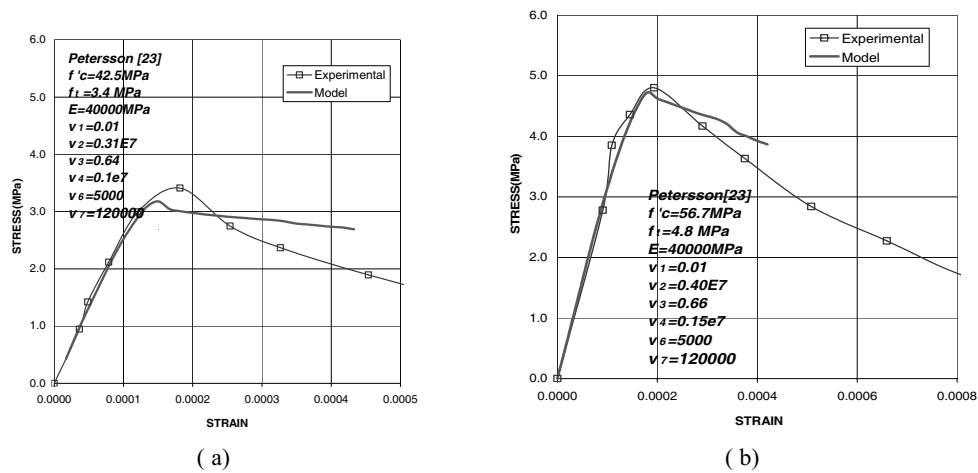

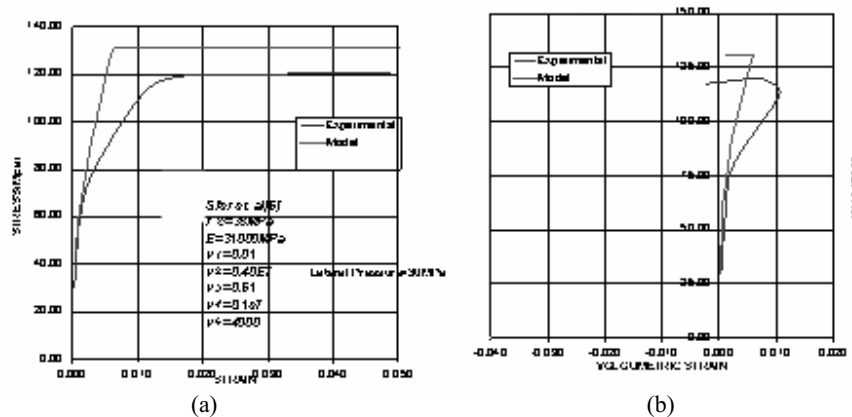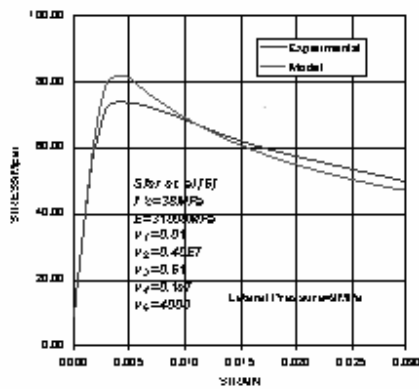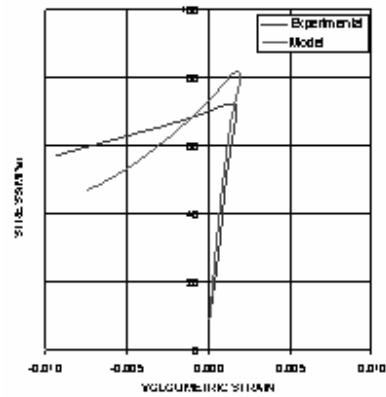**Fig.8** Comparison of model for uniaxial tension experimental data,Petersson[23] a)f'c=42.5 b)f'c=56.7

Fig.9 Comparison of model for Triaxial compression experimental data-High lateral pressure ,Sfer [6] a)Stress-strain curve b)volumetric strain versus stress
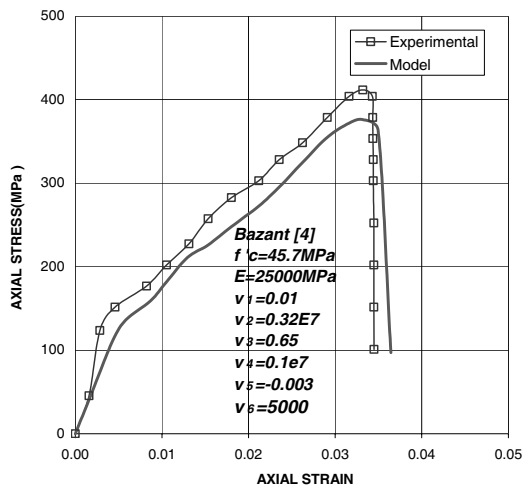
(a)   (b)

Fig.10 Comparison of model for Triaxial compression experimental data-Low lateral pressure ,Sfer [6]
a)Stress-strain curve b)volumetric strain versus stress

Fig.11 Comparison of model for Triaxial compression
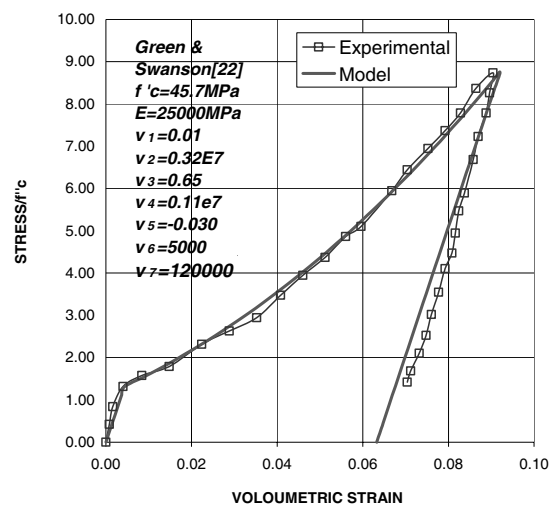experimental data-Axial loading and lateral
unloading,Bazant [4]

Fig.12 Comparison of model for hydrostatic compression
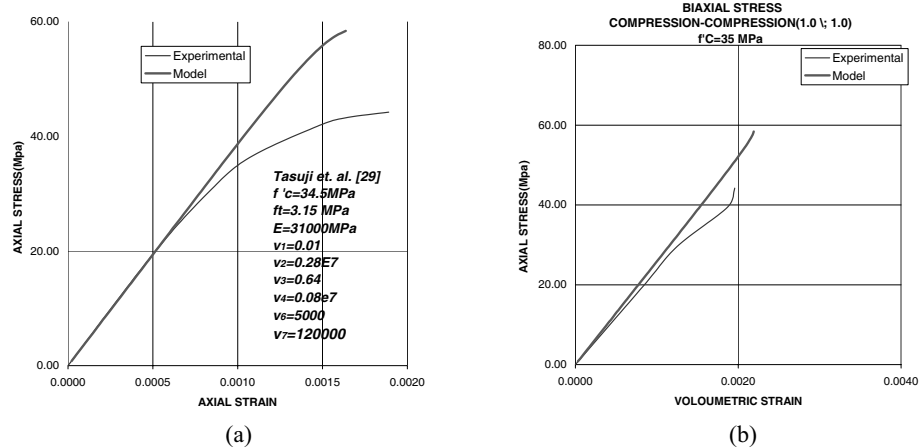experimental data-Green and Swanson [22]

Fig.13 Comparison of model for Biaxial compression-compression experimental data-Tasuji et. al. [29]
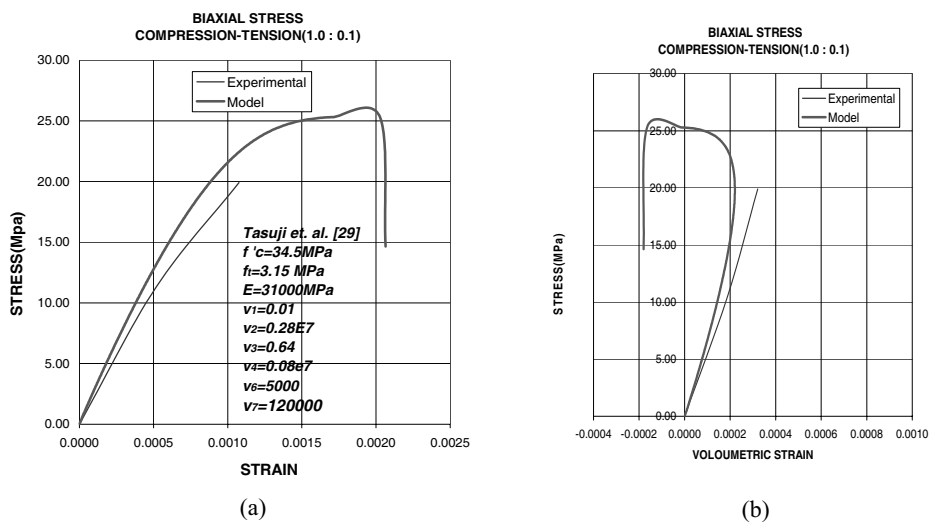a)Stress-strain curve b)volumetric strain versus stress

Fig.14 Comparison of model for Biaxial compression-tension experimental data-Tasuji et. al. [29]
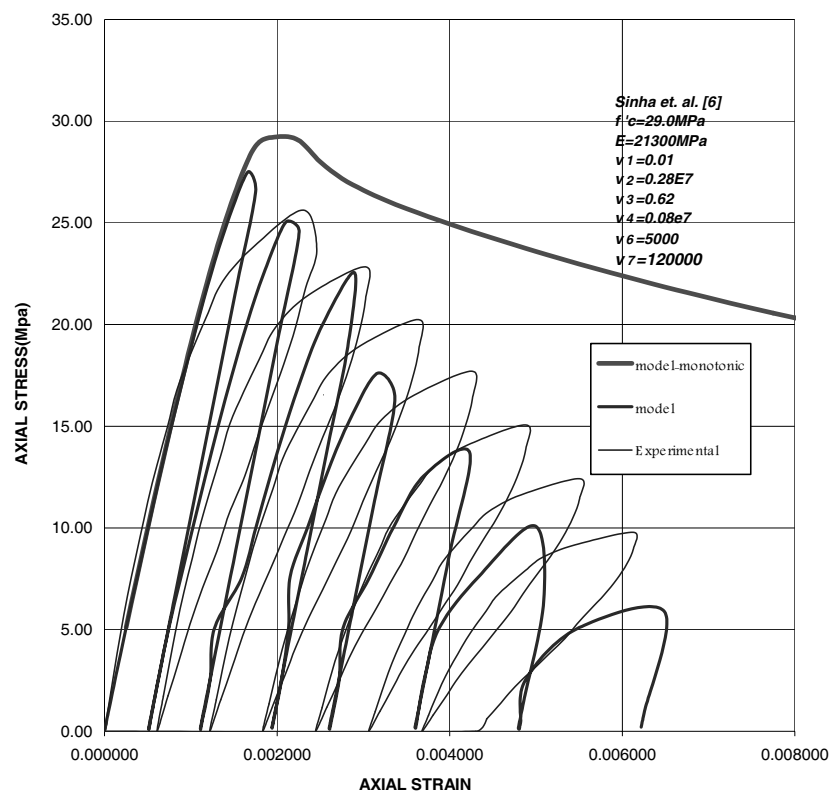a)Stress-strain curve b)volumetric strain versus stress

Sinha et. al. [6]
f 'c=29.0MPa
E=21300MPa
v 1 =0.01
v 2 =0.28E7
v 3 =0.62
v 4 =0.08e7
v 6 =5000
v 7 =120000

- model-monotonic
- model
- Experimental

Fig.15 Comparison of model for cyclic uniaxial compression experimental data-Sinha et. al. [28]
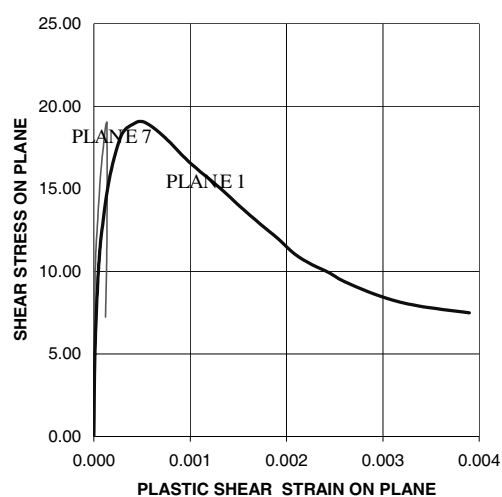

PLANE 7

PLANE 1

Fig.16 Typical Shear stress- plastic strain for different planes in the uniaxial compression test

between model results and test data.

Figure 16 show the shear stress and shear strain diagram for typical planes of 1(similar 2,3 and 4) and plane 7(similar 8,9 and 10) in the uniaxial compression loading, it shows that plane 1 has more plasticity and shear strain than plane 7 because the normal compression stress in plane 1 is larger than plane 7 till peak stress after that in the descending branch plane 1 continues to increase the shear strain but plane 7 that didn't reach the peak stress started to unloading it shows the phenomena of mulilaminate when one plane is under loading the other may be on the unloading, it is more complex when complex load path is considered and the capability of model allows user to simulate any stress/strain load path.

6. Conclusions

From this research on the basis of substructure a model for simulation of concrete behavior under any stress/strain path in the multilaminate framework with using sub-loading surface is derived. However the model has too many parameters but with calibration of 3 to 7 variable parameters it can be able to predict the plastic behavior of normal concrete under any arbitrary load path in ascending/descending branch of loading. The comparison of model with experimental data including uniaxial compression, tension, biaxial loading, triaxial compression, hydrostatic compression and cyclic loading show the good simulation of model.

7. References

[1] Candappa D.C., Sanjayan J.G.,Setunge S., Complete triaxial stress-strain curves of High strength concrete,ASCE-J. of Mat. In civil Eng.2001,vol.13,NO.3,Pages,209-215

[2] Hashiguchi K., Elastoplastic constitutive equations with extended low rules, J .Fac . Agr., Kyushu Univ.1994, NO.38, Pages, 279-286

[3] Lopez cela J.J., Material identification procedure for elastoplastic Drucker-Prager Model _(Technical note), ASCE- J. of Eng. Mech. 2002, vol. 128, NO.5, Pages, 586-591

[4] Bazant Z.P. et. al. Microplane model M4 for concrete (Parts I & II),ASCE J. of Eng. Mech. Sep. 2000,pp944-970

[5] Pietruszczak S. Pande G.N., Multilaminate framework of soil models=Plasticity formulation, 1986, NO., Pages,10

[6] Sfer D., Carol I., Gettu R., Este G., Study of the behavior of concrete under triaxial compression, ASCE-J. of Eng. Mech . 2002, vol. 128, NO. 2, Pages, 156-163

[7] Schmidt R.J.,, Wang D., Hansen A.C., Plasticity Model for Transversely Isotropic Materials, ASCE- J. of Eng. Mech.1993, vol.119,NO.4,Pages,748-766

[8] Stankowski T., Rnesson K., Sture S., Fracture and slip of interfaces in cementitious composites :(pats 1,2), ASCE-J. of Eng. Mech. 1993, vol. 119, NO.2, Pages, 292-325

[9] Palaniswamy R. Shah S.P. Fracture and stress strain relationship of concrete under triaxial compression, ASCE J. of

the structural div.1974, vol.100, NO. ST5, Pages, 901-916

[10] Kotsovos M.D. Newman J.B. A mathematical description of the deformational of concrete under complex loading, Mag. Of concrete research1979, vol.31, NO. 107, Pages, 77-90

[11] Kotsovos M.D. Newman J.B. Generalized stress-strain elations for concrete, ASCE-J. of Eng. Mech. Div.1978, vol.104, NO .EM4, Pages,845-855

[12] Ahmad S.H., Shah S.P. Complete Triaxial stress-strain curves for concrete, ASCE J. of the structural div.1982, vol.108, NO. ST4, Pages, 723-741

[13] Chen R.C., Carrasquillo R.L(1986)., Behavior of high strength concrete under uniaxial and biaxial compression,sp-87-14, Pages,251-273

[14] Shah S.P., Sankar S.P., Internal cracking and stain softening response of concrete under uniaxial compression, ACI mat. J.1987, vol.84, NO.M22, Pages,200-212

[15] Pons G., Ramoda S.A., Maso J.C. Influence of the loading history on fracture mechanics parameters of microconcrete, ACI mat. J.1989, vol.85, NO.M37, Pages,341-346

[16] Tang T., Ouyang C., Shah S.P.A simple method for determining material fracture parameters from peak loads, ACI mat. J.1996, vol.93, NO.2, Pages,147-157

[17] Ansari F. Stress-Strain response of microcracked concrete in direct tension, ACI Mat. J.1987,vol.84,NO.M42,Pages,481-490

[18] Chen W.F.,-Plasticity in reinforced concrete, 1982,McGraw Hill Book co. 474PP.

[19] Shayanfar M.A., Nonlinear finite element analysis of normal and high strength concrete structure, Mc Gill Univ. Ph.D thesis1995

[20] Sadrnejad S.A., A sub-loading surface multilaminate model for elastic plastic porous media, IJE, Vol. 15, No.4, Nov. 2002

[21] Hashiguchi K., Guide-manual for elastoplastic constitutive models Comparison of Elastoplastic Constitutive Models Emphasizing on Subloading surface model and Bounding surface model, Kyushu University website

[22] Green S.J. and Swanson S.R. (1973)Static Constitutive Relation for Concrete Technical Report No. AFWL-TR-72-244(AD-761820) Air Force Weapons Laboratory, New Mexico

[23] Peterson P.E.(1996),"Crack growth and Development of Fracture Zone in Plain Concrete and Similar Materials"Rep. No. TVBM1006 Lund institute of technology.

[24] Bresler B.,Pistler K.S. 'Strength of concrete under combined stresses"J. of Am.Conc. Inst.(1958)551(9)pp321-345

[25] Kupfer H.,Hilsdorf H.K. and rusch H.(1969)'Behavior of concrete under

biaxial stresses"J. of Am.Conc. Inst. (66)pp 656-666

[26] Van Mier J. G.(1984) "Multiaxial strain softening of concrete"J. of Mat. And Fracture vol.111 (19)pp179-200

[27] Grestel K.H. et. al. "Behavior of concrete under multiaxial stress states" ASCE, J. of Eng. Mech., Dec.1980,pp-1383-1403

[28] Sinha B.P.,Gerstel K.H. and Tulin L.G.,"Stress-Strain relations for concrete under cyclic loading"J. Am. Conc. Inst.(1964),62(2)pp 195-210

[29] Tasuji M.E.,Slate F.O.,Nilson A.H.,"Stress-Strain response and fracture of concrete in biaxial loading"ACI J., July 1978,pp 306-312

[30] Zienkewics O.C. and Pande G.N., "Time dependent multi-laminate model of rocks-a numerical study of deformation of rock masses,Int. J. of Numerical and Analytical Methods in Geomechanics"1977,pp-219-247

[31] Pande G.N., Sharma K.G, "Multilaminate

model of clays"-A numerical evaluation of the influence of rotation of principal stress axes" Int. J. for Numerical and Analyt. Meth. in Geomech.1983

[32] Bazant Z.P., Oh B.H."Microplane model for fracture analysis of concrete structures" Proceeding symposium on the international of Non-nuclar Munitions with structures,Us Air force Academy May 1983

[33] Sadrnejad S.A., Pande G.N. "A Multilaminate model for sands,Proceeding of 3rd International symosium on numerical models in Geomechanics "NUMOG III, May 1989 Niagara fall, Canada

[34] Taylor G.I. "Plastic strain in metals" J, of Industrial Metals, 62, 1938, pp307-324

[35] Batdorf S.B. ,Budiansky B. "A mathematical theory of plasticity based on the concept of slip" National Advisory Committee for Aeronautics, TN 1871,1949